

CASE FILE
COPY

THE EFFECTS ON CRUISE DRAG OF INSTALLING REFAN-ENGINE NACELLES ON THE MCDONNELL DOUGLAS DC-9

by J. T. CALLAGHAN, J. E. DONELSON AND J. P. MORELLI

Prepared for
NATIONAL AERONAUTICS AND SPACE ADMINISTRATION
NASA Lewis Research Center
Contract NAS 3-16824

THE EFFECTS ON CRUISE DRAG OF
INSTALLING REFAN-ENGINE NACELLES
ON THE MCDONNELL-DOUGLAS DC-9

by J. T. Callaghan, J. E. Donelson, and J. P. Morelli

MCDONNELL DOUGLAS CORPORATION

prepared for

NATIONAL AERONAUTICS AND SPACE ADMINISTRATION

NASA Lewis Research Center

Contract NAS 3-16814

FOREWORD

The high-speed wind tunnel test described in this report was performed by the Douglas Aircraft Company, Configuration Design Branch - Aerodynamics of the McDonnell Douglas Corporation. The work sponsored by NASA Lewis and reported herein was performed between January and April 1973.

This report has been reviewed and is approved by:



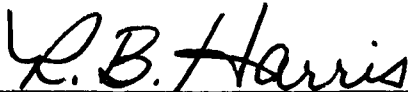
J. E. Donelson
NASA Refan Project Aerodynamicist

Date 5-21-73



F. T. Lynch, Chief
Configuration Design Branch
Aerodynamics

Date 5-21-73



R. B. Harris
Chief Aerodynamics
Engineer for Design

Date 5-23-73



O. R. Dunn
Director of Aerodynamics

Date 5-24-73

TABLE OF CONTENTS

	Page
1.0 SUMMARY	1
2.0 INTRODUCTION	3
3.0 SYMBOLS	7
4.0 APPARATUS AND TESTS	9
4.1 Model Description	9
4.1.1 Basic Model	9
4.1.2 Nacelle Geometry	9
4.1.3 Nacelle Installation Comparison	9
4.2 Test Apparatus	10
4.2.1 Facility and Model Installation	10
4.2.2 Instrumentation	10
4.3 Test Procedure and Data Accuracy	11
5.0 RESULTS AND DISCUSSION	13
5.1 Incremental Drag	13
5.2 Wing Pressures	13
5.3 Nacelle/Pylon/Fuselage Channel Pressures	15
6.0 CONCLUSIONS	17
7.0 REFERENCES	19
8.0 FIGURES	21

1.0 SUMMARY

A high-speed wind tunnel test was conducted in the NASA Ames 11-foot wind tunnel in support of the NASA Refan Program in order to assess the performance aspects of installing a larger refan-engine nacelle on the DC-9-30. The test was prompted by the fact that the refan nacelle is about 22-percent larger in diameter relative to the production nacelle and, if the current pylon were used, the increased span of the nacelle and pylon could decrease low-speed deep-stall recovery margin. One of the ways to minimize this effect is to install the nacelle closer to the fuselage with a pylon of shorter span, but this would introduce a potential interference drag problem at cruise speeds. The purpose of this test was to examine the effect of the larger nacelle and of the nacelle-fuselage lateral spacing on cruise drag.

Analysis of the results from the test leads to the following conclusions:

1. At the lower Mach numbers ($M_0 < 0.7$), the drag increment of the refan installation relative to the production nacelle and pylon installation is equal to that calculated by considering only the wetted area and form factor changes.
2. At typical cruise Mach numbers ($M_0 \approx 0.78$) there exists a favorable interference drag relative to the calculated difference between the refan and production installations. This amounts to about 2-percent of total airplane drag for the Series 30 installation. Applying this favorable effect to the full-scale installation, where the skin friction penalty due to the larger nacelle amounts to about 2-percent of total airplane drag, would result in the refan nacelle being installed without any drag penalty.
3. This favorable effect most likely occurs because the positive pressures on the stream tube entering the engine suppress the wing upper-surface velocities, thereby moving the wing shock forward and reducing the Mach number at the shock with subsequent reduction in wing compressibility drag (the stream tube is larger and located farther forward with the refan installation). This effect would be expected to be even larger for a Series 10 airplane (inlet located closer to wing), but slightly less for a Series 40 (inlet located farther aft of wing).

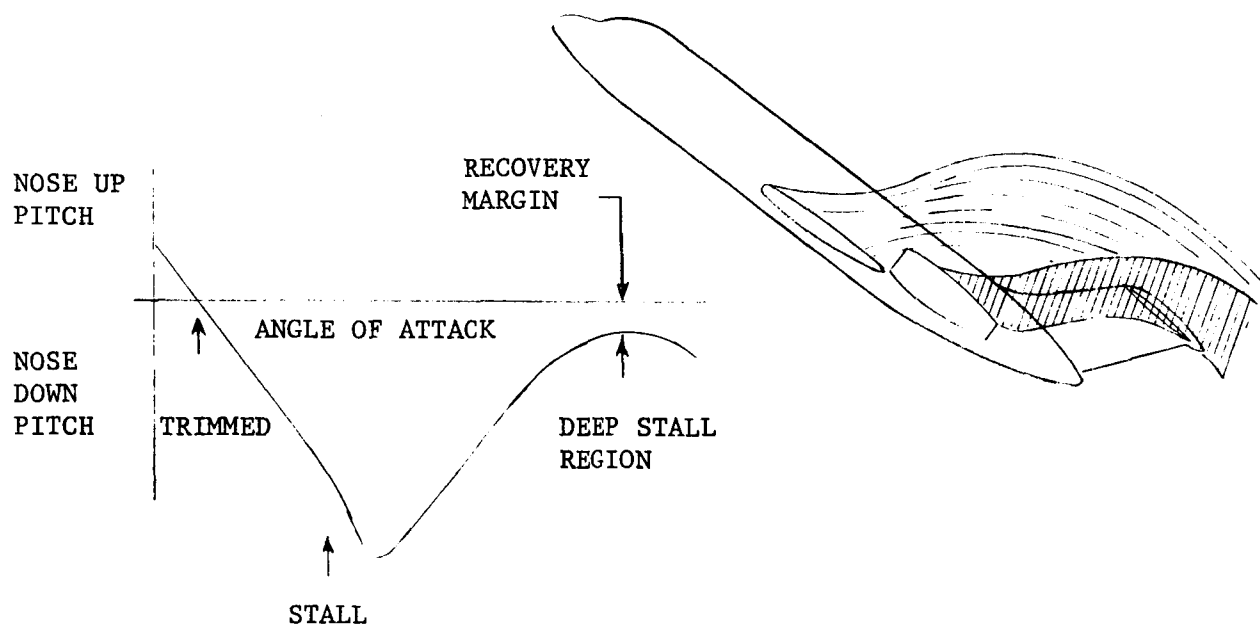
4. There is little effect of pylon span on the incremental drag of the refan installation. The incremental drags for the 5.2- and 11.0-inch span pylons are about the same while the 16.7-inch span pylon is about one drag count ($\Delta C_D = 0.0001$) less at 0.78 Mach number.
5. The nacelle/pylon/fuselage channel does not exhibit any excess supersonic velocities or lack of recompression. The refan inlet is long enough to prevent superposition of the cowl- and pylon-peak pressure coefficients.

This test was made in conjunction with a low-speed test in the NASA Ames 12-foot Facility to examine the effects of the larger nacelle on deep-stall recovery. The results of the low-speed test are summarized in a separate report.

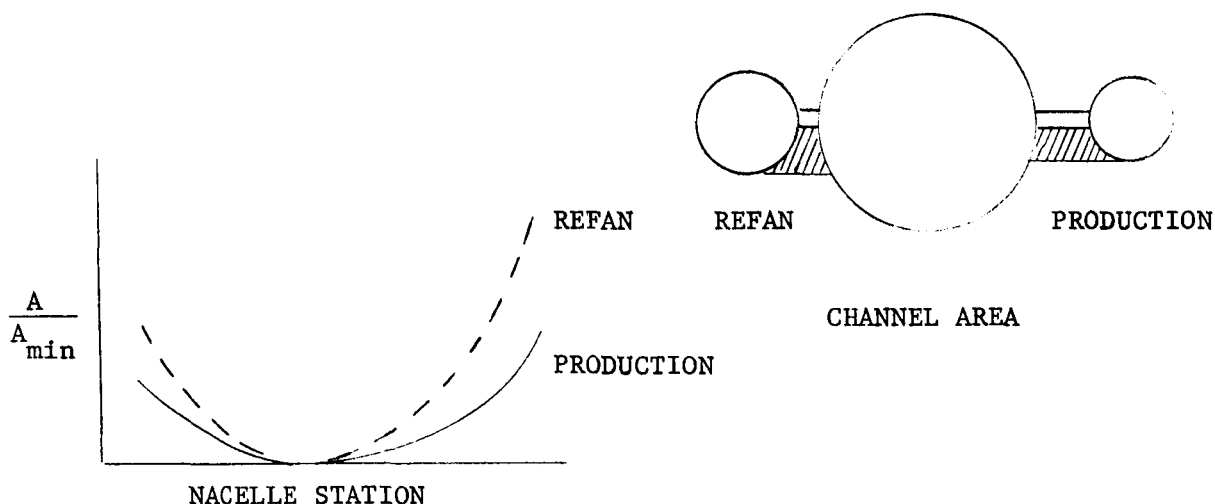
2.0 INTRODUCTION

The aft fuselage-mounted engine installation on the DC-9 is similar to other installations of this type. The particular geometry used on the DC-9 was developed with major consideration given to the effects on (1) cruise drag, (2) deep stall recovery, (3) minimum control speeds and (4) nacelle/pylon accessibility. The present installation is essentially interference-drag free, that is, there is little or no excess drag due to sonic velocities (wave drag) or excess adverse pressure gradients (pressure drag). The installed nacelle and pylon drag, therefore, consists almost entirely of basic skin friction and form drag.

While it would be desirable to install the larger-diameter refan nacelle on the existing pylon, this would increase the span of the nacelle/pylon combination, thus creating a potential low-speed deep-stall problem. With aft-fuselage mounted nacelles there exists what is called a deep stall region where the wake from the nacelles and pylons can blanket the horizontal tail and reduce its effectiveness and therefore reduce nose down pitch control. While this happens well beyond the stall, and outside the normal operating regime, it has been the position of the Douglas Company to provide positive aerodynamic recovery and not rely on mechanical devices to prevent deep stall entry. This phenomenon is illustrated in the sketch below.



With the larger nacelle diameter associated with the refan engine (≈ 22 percent), there was a concern that the increased span of the nacelle and pylon would further reduce the tail effectiveness and decrease or negate the existing recovery margin. A way of reducing the span would be to position the nacelle closer to the fuselage using a pylon of shorter span. Initial studies showed that with some reduction in pylon accessibility the 11.5-inch increase in nacelle diameter could all be offset by a shorter-span pylon, thereby keeping the outer nacelle line the same as the existing nacelle. This would require reducing the channel width from 16.7 to 5.2 inches. The following sketch shows the change in channel area distribution with the snugged-in nacelle.



With the refan installation there is more channel area convergence and divergence. This was a concern because of the possibility of interference drag at cruise speeds. The higher degree of channel divergence could lead to increased adverse pressure gradients in the channel area. The result of these increased gradients would be thickening of the nacelle/fuselage/pylon boundary layer with consequent drag increase due to momentum loss and possibly boundary layer separation. A second source of interference drag may occur if the velocities in the channel become supersonic. This can result in shock wave drag and possible shock-induced boundary layer separation.

In order to investigate the potential interference drag problem a high-speed wind tunnel test was conducted during January 1973 in the NASA Ames 11-foot

wind tunnel. The purpose of this test was to determine the incremental drag of the refan nacelle installation as a function of nacelle lateral spacing. Channel spacings from 16.7 inches (existing) to 5.2 inches were examined.

The pertinent test results are analyzed and discussed in this report. The results from this test were incorporated in the selection of the pylon spacings tested in a low-speed test at the NASA Ames 12-foot wind tunnel to investigate the deep-stall recovery aspects of the refan installation. The results of that test are reported in Reference 1.

3.0 SYMBOLS

$\frac{A}{A_{\min}}$	Ratio of local channel cross-sectional area to minimum value
$b/2$	Wing semi-span normal to plane of symmetry
C	Wing chord at location of pressure orifices, inches
C_D	Airplane drag coefficient, $\text{Drag}/q_o S_w$
ΔC_D	Incremental drag coefficient
C_L	Airplane lift coefficient, $\text{Lift}/q_o S_w$
C_P	Pressure coefficient, $\frac{P_L - P_o}{q_o}$
ℓ_i	Inlet length (from engine face), inches
L	Nozzle length, inches
L/H	Nozzle length-to-height ratio
M_L	Local Mach number
M_o	Freestream Mach number
P_L	Local static pressure, psf
P_o	Freestream static pressure, psf
q_o	Freestream dynamic pressure, $0.7 P_o M_o^2$, psf
S_w	Wing reference area, sq ft
X	Distance from wing leading edge, inches
y	Pylon span, inches

4.0 APPARATUS AND TESTS

4.1 MODEL DESCRIPTION

4.1.1 Basic Model

The model is a 6-percent scale representation of the DC-9-30 and is designated LB-151M. A three-view drawing of the DC-9-30 with the refan-engine nacelle is shown in Figure 1. The model was tested with the horizontal and vertical tail removed. The fuselage, wing, and production nacelles and pylons have been previously tested in the Ames Facility. The refan nacelles and pylons were fabricated for this test program.

4.1.2 Nacelle Geometry

Because of the larger fan diameter of the JT8D refan engine (higher bypass ratio), the nacelle required to enclose the engine and accessories is also larger. The planform diameter is about 11.5 inches larger than the existing nacelle (≈ 22 percent). The nacelle geometry simulated for this test is based on the intermediate treatment level shown in the first-submittal NAID document (Reference 2). The refan nacelle geometry has the following characteristics:

1. The inlet length from the engine face to the highlight is 43.0 inches.
2. The maximum nacelle diameter is 64.0 inches (plan view).
3. The nozzle L/H is 4.30 (L = 75.0 inches).
4. The overall nacelle length is 253.0 inches.
5. The nacelle is of long duct design very similar in overall appearance to the existing production nacelle.
6. The stang fairings required to enclose the thrust reverser operating linkage are simulated.
7. The afterbody boattail angle is 13.0 degrees.

A dimensional sketch of the refan nacelle compared to the baseline nacelle is presented in Figure 2.

4.1.3 Nacelle Installation Comparison

The installation of the refan nacelle compared to the production nacelle is shown in Figure 3. The pylon incidence is the same for both installations.

The inlet leading edge (highlight) is located 30 inches further forward and the nozzle is located 21.5 inches further aft. The model provided for three nacelle/pylon spacings described below:

1. P₁₆, y = 16.7 inches - existing production pylon with the inside refan nacelle line coincident with the existing nacelle line.
2. P₁₄, y = 5.2 inches - stub pylon with the outside refan nacelle line coincident with the existing nacelle line. The planform span of the refan nacelle and pylon is the same as the production installation.
3. P₁₅, y = 11.0 inches - intermediate spacing to account for the possibility that (1) the 5.2-inch pylon causes an excessive drag penalty or (2) due to accessibility constraints the 5.2-inch pylon is not possible to build.

4.2 TEST APPARATUS

4.2.1 Facility and Model Installation

The NASA Ames Research Center 11- by 11-foot continuous-flow, variable-density transonic wind tunnel was used for this test program.

The model installation is shown in Figure 4. The fuselage is supported by a blade sting that enters the top of the model forward of the wing-fuselage intersection. This allows the model to be tested free of interference from the conventional sting arrangement, since the area of interest is the fuselage afterbody and the surrounding components. The fuselage nose has been shortened 133.3 inches (full scale) to achieve the proper boundary layer thickness at the nacelle location. A photo of the model installed in the wind tunnel is shown in Figure 5.

4.2.2 Instrumentation

The model was equipped for measuring both force and pressure data. The model instrumentation consisted of a six-component internal balance, a six-valve scanivalve module, and a dangleometer angle-measuring device. This electronic equipment was used to measure the model forces, static pressures on the wing, fuselage, pylons, and nacelles, and to measure model angle of attack.

The model was mounted on the Task 2.5-inch diameter Mark XIA internal strain gage balance. The balance was installed backward, with respect to the model, in the DAC 5759797 blade sting assembly. The blade sting was inserted into the Ames straight adaptor, which was mounted on the Ames 40-inch extension which, in turn, was mounted on the pitch pod. The balance cavity in the fuselage center body is at a one degree angle to the fuselage reference plane such that, when the balance is at zero angle of attack, the model is at +1.0 degree angle of attack. This allows the measurement of drag to be made primarily on the balance axial force beam when the model is at the cruise angle of attack.

The model was aligned in pitch by means of a machined surface beneath a cover plate on the fuselage center body in the area of constant cross-section. The model alignment in roll was checked by measurements from the wing tips to the tunnel floor. The angle-measuring device was mounted in the nose of the model and used for setting angle of attack. This equipment, along with the internal balance, was provided by NASA Ames.

The pressure instrumentation details are shown in Figure 6. Static pressure orifices are located on the wing at two semispan locations (17 and 38 percent), and in the fuselage/pylon/nacelle upper and lower channels. The wing inboard row (17 percent) is inboard of the engine centerline and the outboard row (38 percent) is outboard of it.

One row of static pressure orifices is located on the fuselage, nacelle, and pylon for both the upper and lower channels. Spacing is such to be sufficient to detect the effects of nacelle size-and-spacing changes on channel velocities and gradients. In addition, the lower-channel fuselage pressure orifices extend to the tail cone to examine the effects on fuselage afterbody recompression.

4.3 TEST PROCEDURE AND DATA ACCURACY

The test was conducted at a constant Reynolds number of 8 million per foot (5.9×10^6 on the mean aerodynamic chord) through a Mach number range from

0.70 to 0.82. The Reynolds numbers at Mach numbers of 0.50 and 0.60 were reduced to 6.2 and 7.2 million per foot, respectively, (4.6 and 5.3×10^6 on mean aerodynamic chord) because of the operating envelope of the tunnel. The Reynolds number was held to within $\pm 100,000$ and the Mach number to within ± 0.002 . Angle of attack was varied at each Mach number in one-half degree increments over a range corresponding to lift coefficient values between zero and 0.5. The angle of attack tolerance is ± 0.1 degrees of the indicated value. Selected Mach numbers were repeated to ensure the validity of the data. The data repeatability was excellent throughout the test (C_D repeated within ± 0.0001). The pressure data were gathered at enough Mach numbers to provide the necessary information for understanding any potential interference problems. All data were gathered with the horizontal and vertical tails removed.

5.0 RESULTS AND DISCUSSION

5.1 INCREMENTAL DRAG

Figure 7 shows the incremental drag difference between the refan installation and the production installation. Two pylon spans for the refan nacelle are shown ($y = 16.7$ inches and $y = 5.2$ inches). The increment is shown versus Mach number for the lift coefficients of operational interest ($0.25 - 0.4$). It can be seen that for the lower Mach numbers where the aircraft is free of compressibility effects ($M_0 < 0.7$), the measured increment is about as estimated considering only the internal and external skin friction and form drag of the larger flow-through nacelle. For Mach numbers greater than 0.7 the increment is less than the estimate. This trend is apparent over the operational range of lift coefficients. At a typical cruise condition of $M_0 = 0.78$, $C_L = 0.35$ the favorable effect amounts to approximately 2-percent of the airplane drag ($\Delta C_D = 0.0005$). This compares closely to the calculated penalty (due only to increased external wetted area) for the full-scale intermediate-treatment configuration (Reference 2) at flight conditions, which would say that the refan nacelle can be installed without paying a drag penalty due to the larger nacelle. The fact that Figure 7 still shows a small penalty for the refan nacelle at this condition is due to the increased skin friction drag at the model Reynolds number and due to the incremental internal drag of the flow-through nacelle.

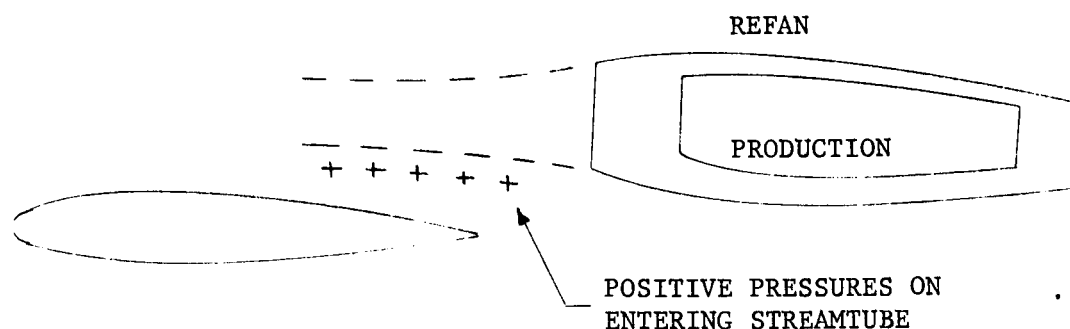
Figure 8 shows that there is little effect of pylon spacing on the drag increment. For $M_0 = 0.78$ the favorable increment exists for all three pylon spacings, and is slightly greater for the 16.7-inch spacing (about one drag count, $\Delta C_D = 0.0001$).

These results require examination of the pressure data to understand the mechanism that caused this favorable interference.

5.2 WING PRESSURES

The fact that the drag reduction is Mach number dependent indicates that it must be a reduction in compressibility drag. Wing surface pressures were measured at two semi-span locations - 17-percent $b/2$ (inboard of the nacelle

location), and 38-percent $b/2$ (outboard of the nacelle location). Figure 9 shows the upper-surface pressures as a function of Mach number for the various nacelle configurations tested. While only the typical cruise lift coefficient ($C_L = 0.35$) is shown, the same general trends exist at other lift coefficients. Figure 9 shows that at the lower Mach numbers ($M_0 = 0.5$ shown) there is a general suppression of the upper surface pressures (velocities) with the refan installation relative to the production installation. As the Mach number increases beyond 0.7 this suppression lowers the peak velocities ahead of the shock wave and moves the shock forward thereby reducing the strength of the shock wave and hence the wing compressibility drag. Note also from Figure 9 that the influence of the entering stream tube is felt considerably outboard indicating that it influences the shock over a significant portion of the wing. The following sketch shows how the inlet can influence the wing



pressures. The stream tube of air entering the inlet must slow down as it approaches the inlet since the inlet Mach number is less than the free stream Mach number. This requires positive pressures on the entering stream tube. It is these positive pressures that effect the wing shock. The stream tube for the refan nacelle is larger in diameter (22 percent) and the inlet is considerably longer (30 inches) relative to the production nacelle which places the positive pressures closer to the wing where they have a larger influence. Note from Figure 9 that there is some influence of the basic nacelle, but much less than that for the refan nacelle. These results are also substantiated

by results from a recent flight test program for another DC-9 acoustic-nacelle installation. The inlet was longer and the program was conducted on a Series 10 aircraft which has a shorter fuselage. While the nacelle was no bigger in diameter than the production nacelle the inlet was closer to the wing relative to the refan installation. A favorable interference effect with Mach number was measured and was very similar in both magnitude and characteristics to that measured with the refan installation.

The favorable interference would be expected to be larger for a Series 10 aircraft (shorter fuselage placing the inlet closer to the wing) and slightly less for a Series 40 aircraft (longer fuselage placing the inlet farther from the wing). In addition, since the tested configuration was based on a ringed inlet, if a longer no-ring inlet is selected for the Phase 2 flight test program the indicated improvement will probably be a little larger.

5.3 NACELLE/PYLON/FUSELAGE CHANNEL PRESSURES

Figures 10 and 11 show the pressure distributions in the lower- and upper-nacelle/pylon/fuselage channels for Mach numbers of 0.7 and 0.78. The nacelle and fuselage pressure peaks at about station 900 (Figure 10) are due to the spillage around the cowlings. The cowlings are designed to spill flow with some supersonic velocities. While the peak velocities tend to be aggravated by the closer spacing, they are just sonic at 0.78 Mach number for the 5.2-inch spacing and are subsonic for both the 11.0 and 16.7-inch spacings.

The peak pressures on the inlet cowl are far enough forward that they do not add to the peak pressure on the pylon.

For the upper channel (Figure 11), the leading-edge pylon pressures show local Mach numbers from 1.1 to 1.2 at 0.78 Mach number. However, these high velocities are very localized. Note that the adjoining velocities on the fuselage and nacelle at the same station are both subsonic. Also note that the channel recompressions are all about the same and give no indication of any separation. The recompressions on the aft fuselage were essentially the same for all configurations tested. While Figures 10 and 11 are shown only for $C_L = 0.35$, the pressure distributions for other lift coefficients of interest show the same general trends.

6.0 CONCLUSIONS

From the results of a high-speed wind tunnel test conducted to assess the drag increments for installing a larger refan-engine nacelle installation on the DC-9-30, the following conclusions are drawn:

1. At the lower Mach numbers ($M_0 < 0.7$), the drag increment of the refan installation relative to the production nacelle and pylon is equal to that calculated by considering only wetted area and form factor changes.
2. At typical cruise Mach number ($M_0 = 0.78$) there exists a favorable interference drag relative to the calculated difference between the refan and production installations. This amounts to about 2-percent of total airplane drag for the Series 30. Applying this favorable effect to the full-scale installation, where the skin friction penalty due to the larger nacelle amounts to about 2-percent of total airplane drag, would result in the refan nacelle being installed without any drag penalty.
3. This favorable effect occurs because the positive pressures on the stream tube entering the engine suppress the wing upper-surface velocities thereby moving the wing shock forward with subsequent reduction in wing compressibility drag (the stream tube is larger and located further forward with the refan installation). This effect would be expected to be larger for a Series 10 airplane (inlet located closer to wing) and slightly less for a Series 40 (inlet located farther aft of wing).
4. There is little effect of pylon span on the incremental drag of the refan installation. The incremental drags for the 5.2- and 11.0-inch span pylons are about the same while the 16.7-inch pylon is about one drag count ($\Delta C_D = 0.0001$) less at 0.78 Mach number.
5. The nacelle/pylon/fuselage channel does not exhibit any excess supersonic velocities or lack of recompression. The refan inlet is long enough to prevent superposition of the cowl- and pylon-peak pressure coefficients.

7.0 REFERENCES

1. Doss, P. G.: The Results of a Low-Speed Wind Tunnel Test to Investigate the Effects of Installing Refanned JT8D Engines on the McDonnell-Douglas DC-9. Douglas Report MDC J5961, June 1973.
2. Anonymous: Program on Ground Test of Modified Quiet Clean JT3D and JT8D Engines in Their Respective Nacelles. DC-9-32 Engine and Nacelle/Airframe Integration Definition. Douglas Report MDC J5733, 15 March 1973.

8.0 FIGURES

FIGURE	TITLE
1	DC-9-30 with refan engine installation.
2	Nacelle geometry.
3	Nacelle installation comparison.
4	Wind tunnel model installation.
5	Photo of model installation.
6	Wing- and nacelle/pylon/fuselage-pressure instrumentation.
7	Incremental drag coefficient for refan nacelle.
8	Effect of pylon span on incremental drag coefficient for refan nacelle.
9	Wing upper-surface pressure distributions.
10	Nacelle/pylon/fuselage lower-channel pressure distributions.
11	Nacelle/pylon/fuselage upper-channel pressure distributions.

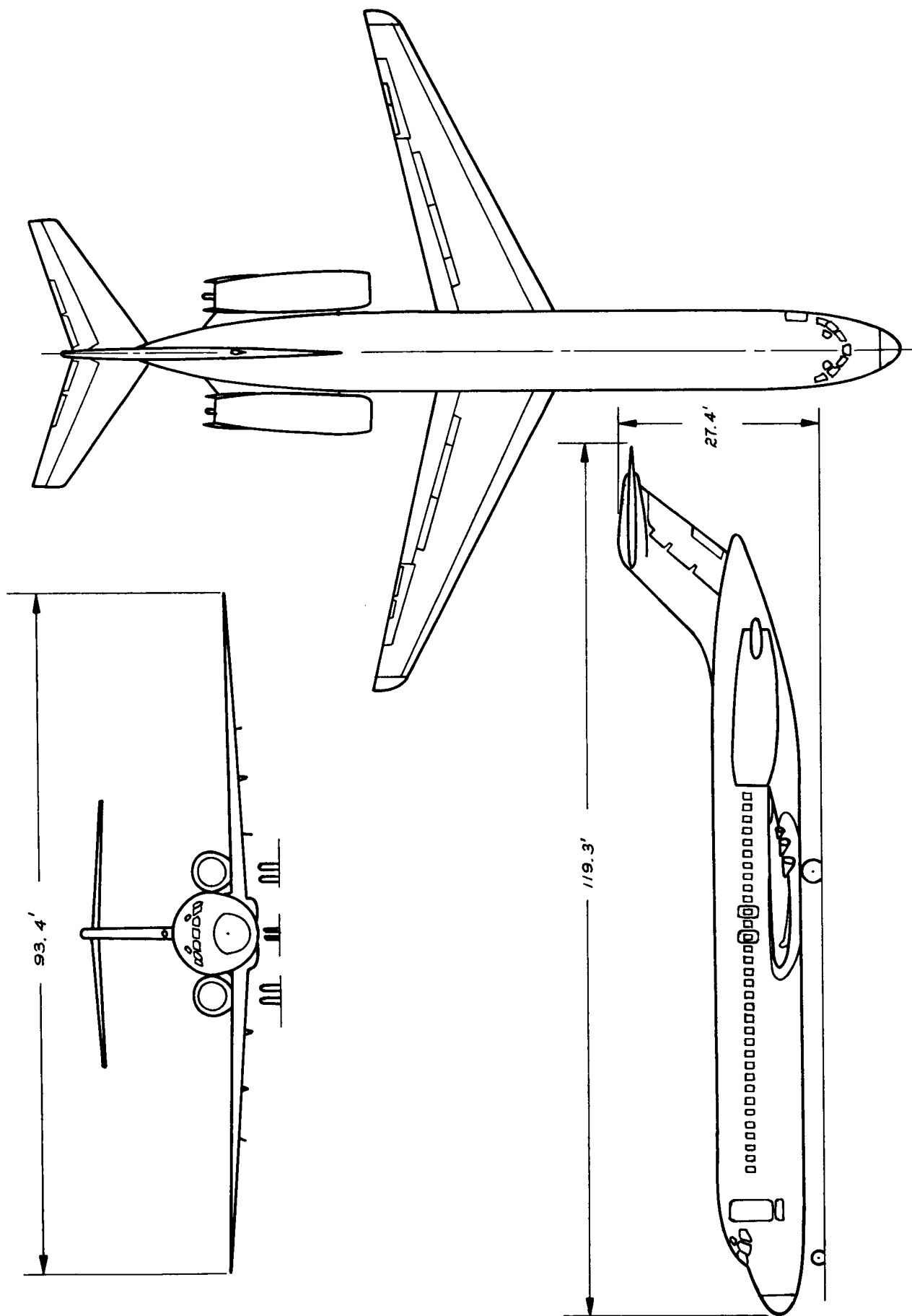
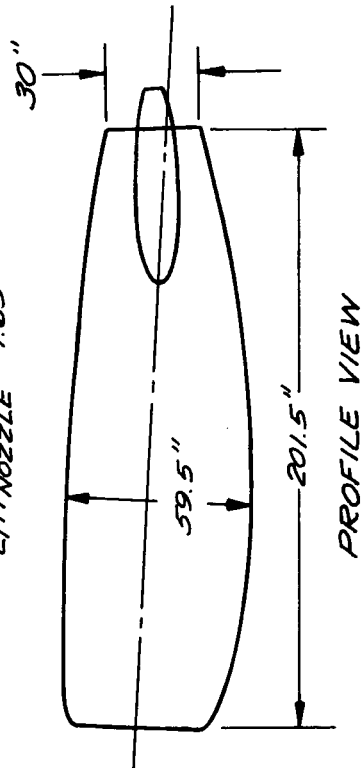


Figure 1.- DC-9-30 with refan engine installation.

PRODUCTION NACELLE (JT8D-9)

REFAN NACELLE (JT8D-109)

$L_i = 28$ INCHES
 $L/H_{NOZZLE} = 1.65$



$L_i = 43$ INCHES
 $L/H_{NOZZLE} = 4.30$

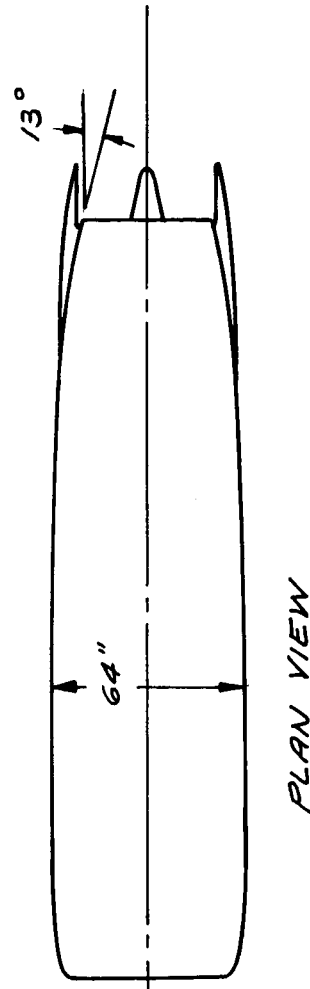
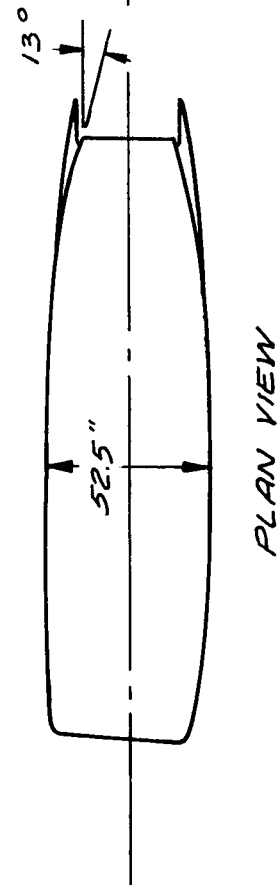
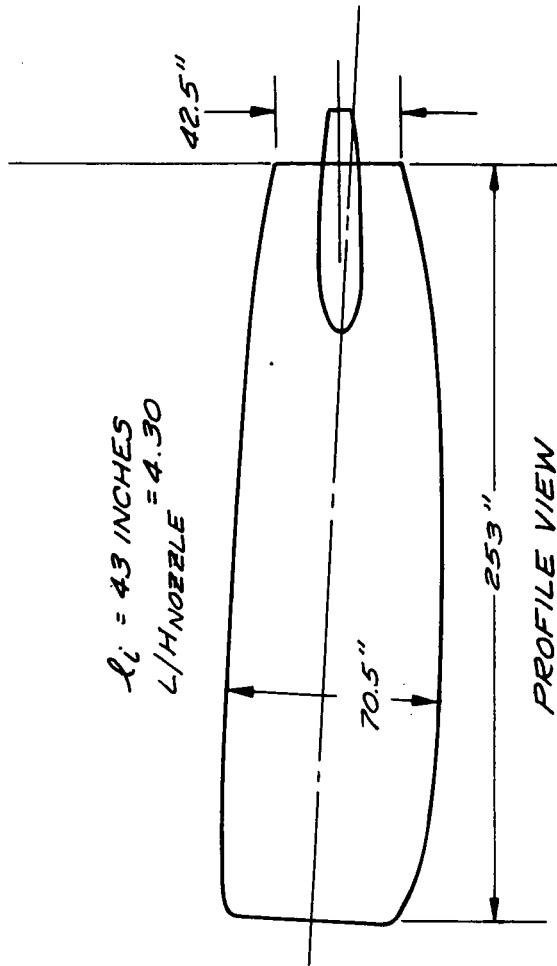
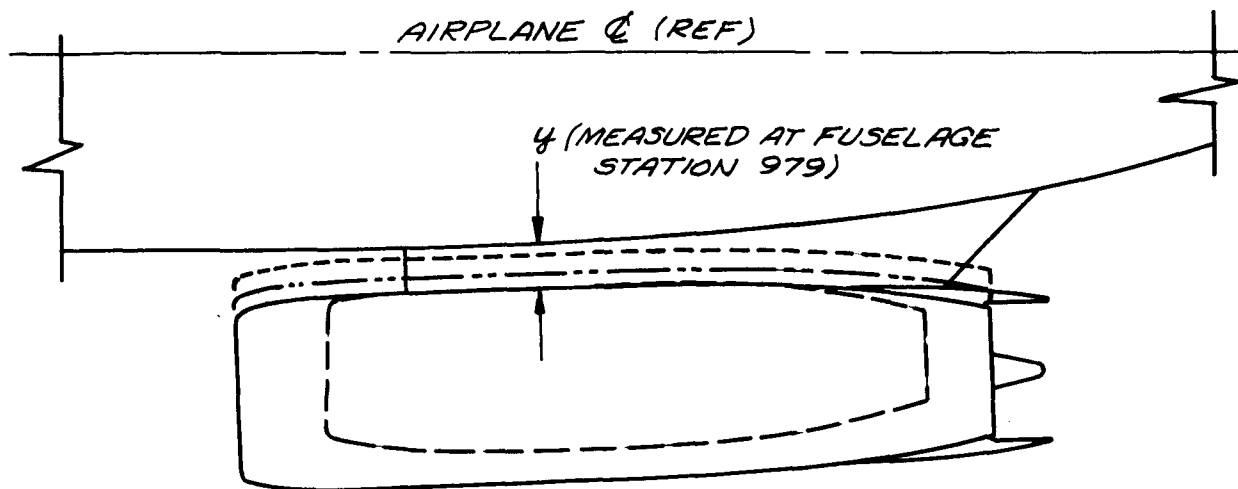
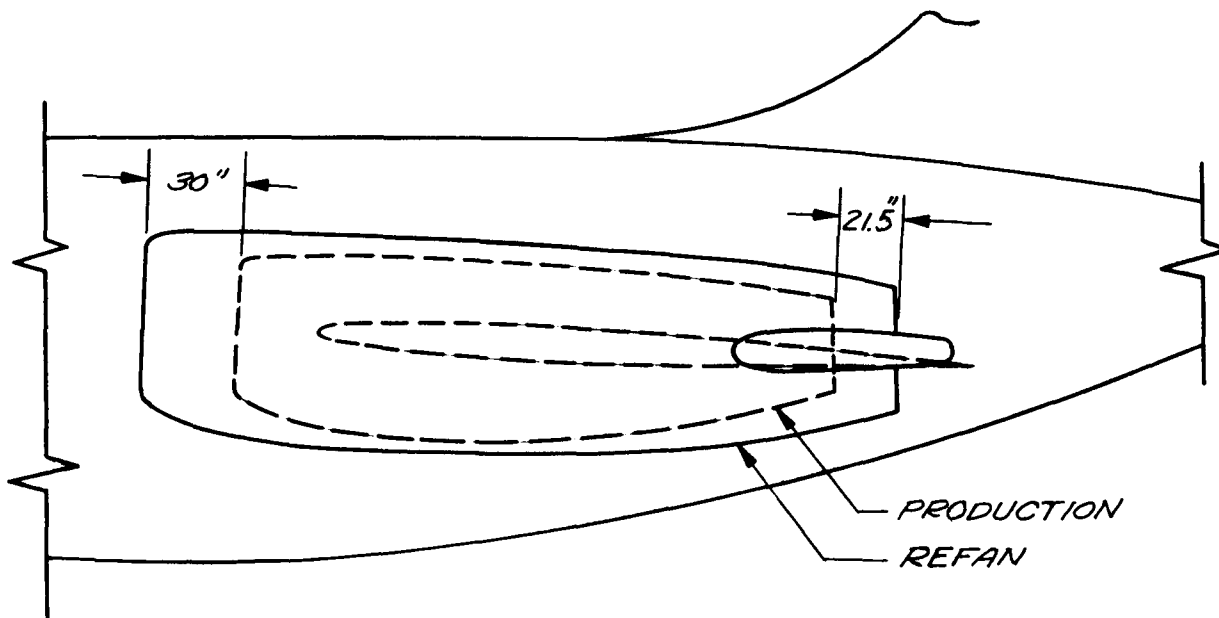


Figure 2.- Nacelle geometry.



	NACELLE	PYLON SPAN y, INCHES
---	PRODUCTION	16.7
---	REFAN	16.7
---	"	11.0
---	"	5.2

PLAN VIEW



PROFILE VIEW

Figure 3.- Nacelle installation comparison.

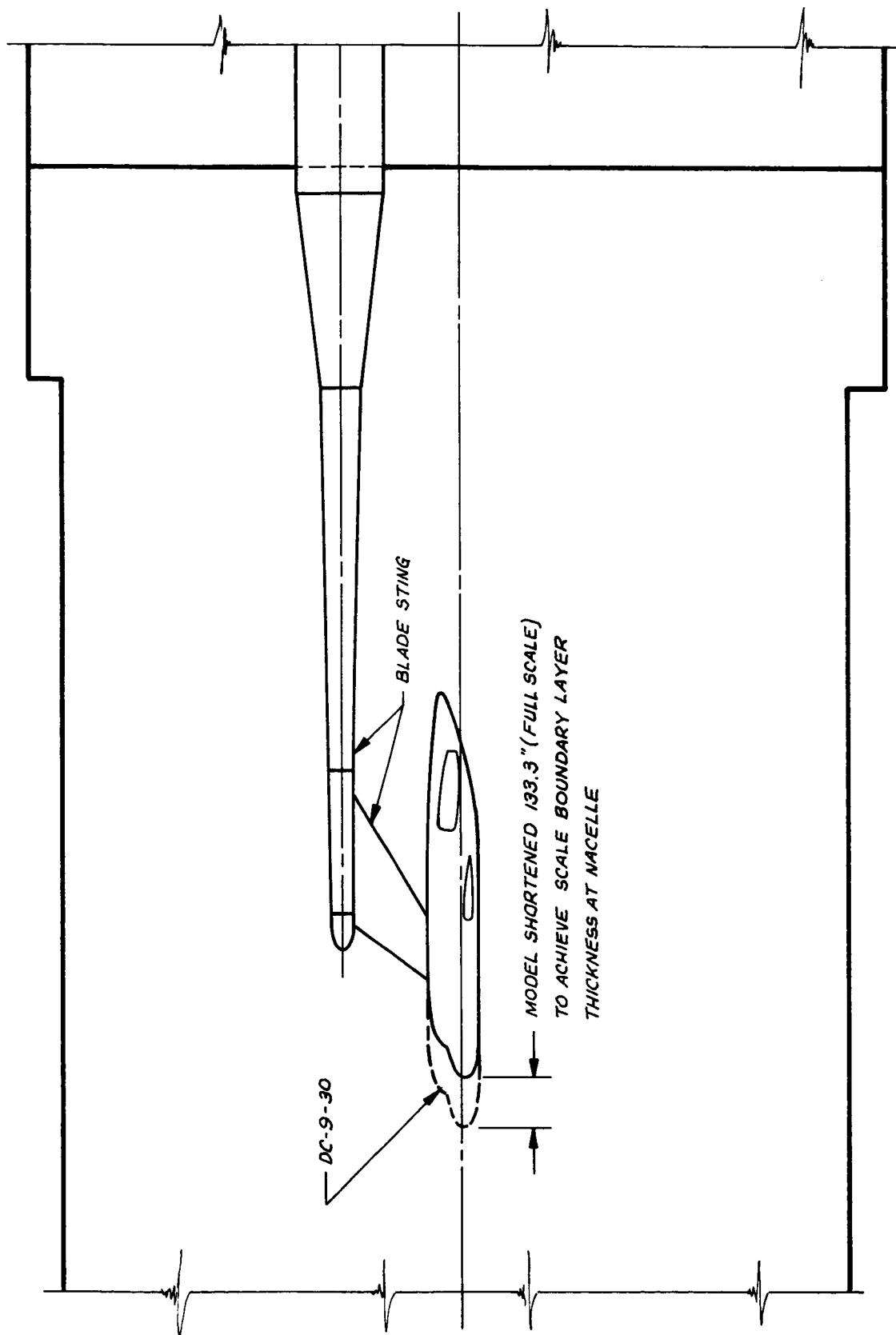
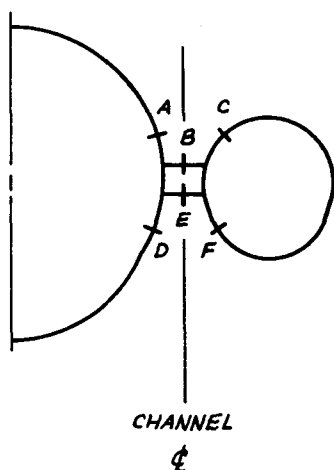
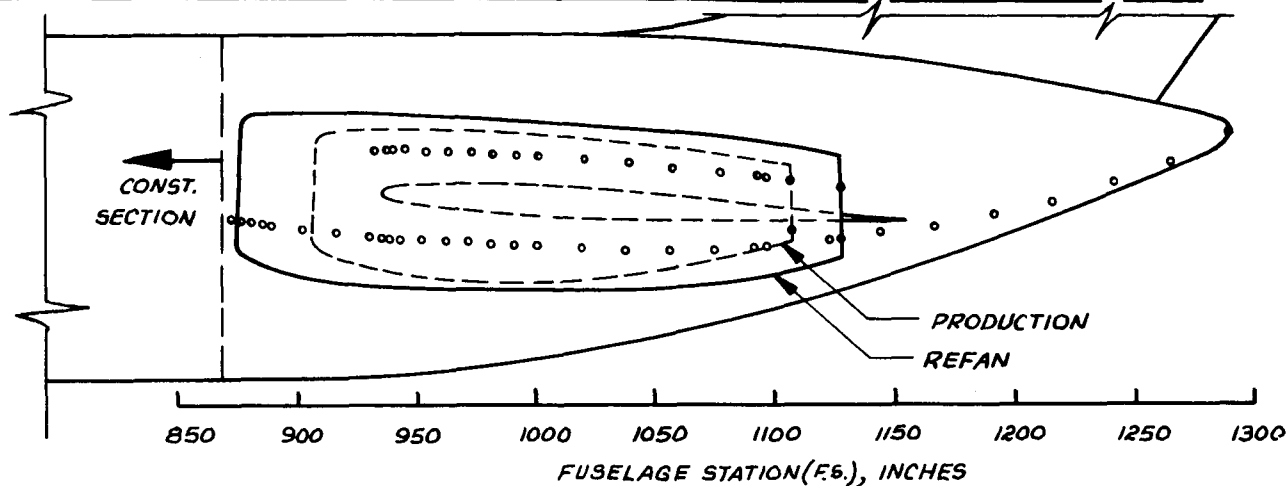


Figure 4.- Wind tunnel model installation.



Figure 5.- Photo of model installation.

NACELLE - PYLON - FUSELAGE CHANNEL PRESSURE ORIFICE LOCATIONS



ROW	NUMBER OF ORIFICES / EXTENT OF ROW	
	PRODUCTION	REFAN
A	15 / F.S. 932.5 TO 1097.5	SAME AS PRODUCTION
B	14 / F.S. 937 TO 1126	14 / F.S. 937 TO T.E. *
C	15 / F.S. 932.5 TO 1106.5	15 / F.S. 932.5 TO 1128
D	30 / F.S. 873 TO 1291	SAME AS PRODUCTION
E	14 / F.S. 937 TO 1126	14 / F.S. 937 TO T.E. *
F	16 / F.S. 917 TO 1107	20 / F.S. 877.5 TO 1129
* T.E. AT F.S. { 1133 FOR 5.2 INCH PYLON SPAN 1130 FOR 11.0 INCH PYLON SPAN 1126 FOR 16.7 INCH PYLON SPAN		

WING PRESSURE ORIFICE LOCATIONS

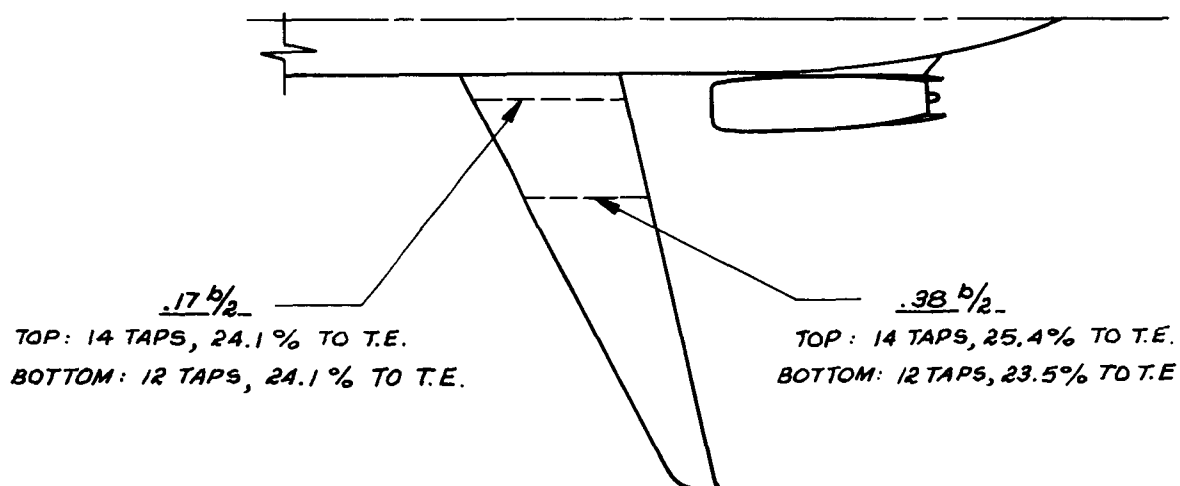


Figure 6.- Wing- and nacelle/pylon/fuselage-pressure instrumentation.

$$\Delta C_D = C_{D_{REFAN}} - C_{D_{PRODUCTION}}$$

$b = 5.2$ INCHES

$b = 16.7$ INCHES

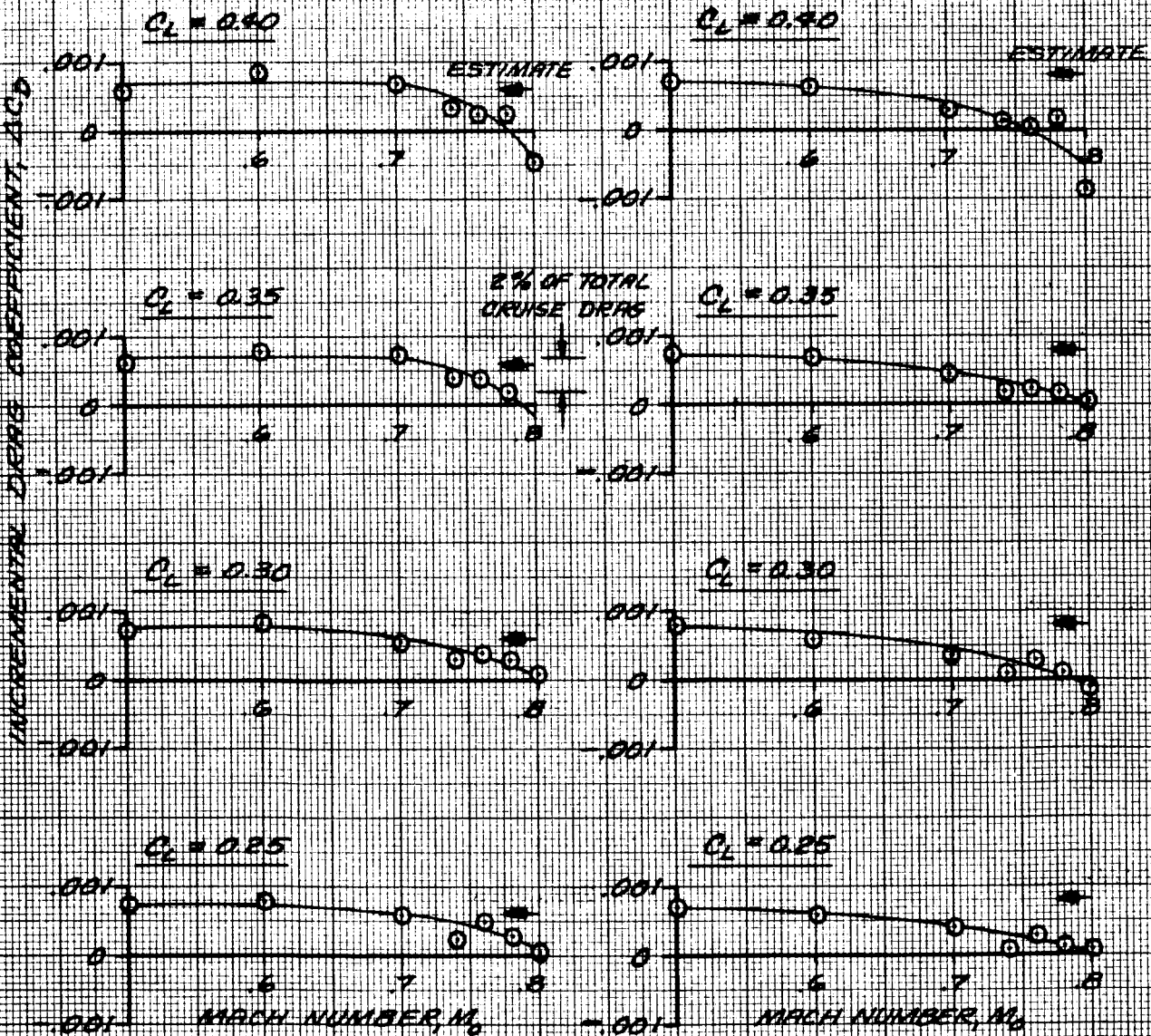


Figure 2.- Incremental drag coefficient for refan nacelle.

$$\Delta C_D = C_{D_{REFAN}} - C_{D_{PRODUCTION}}$$

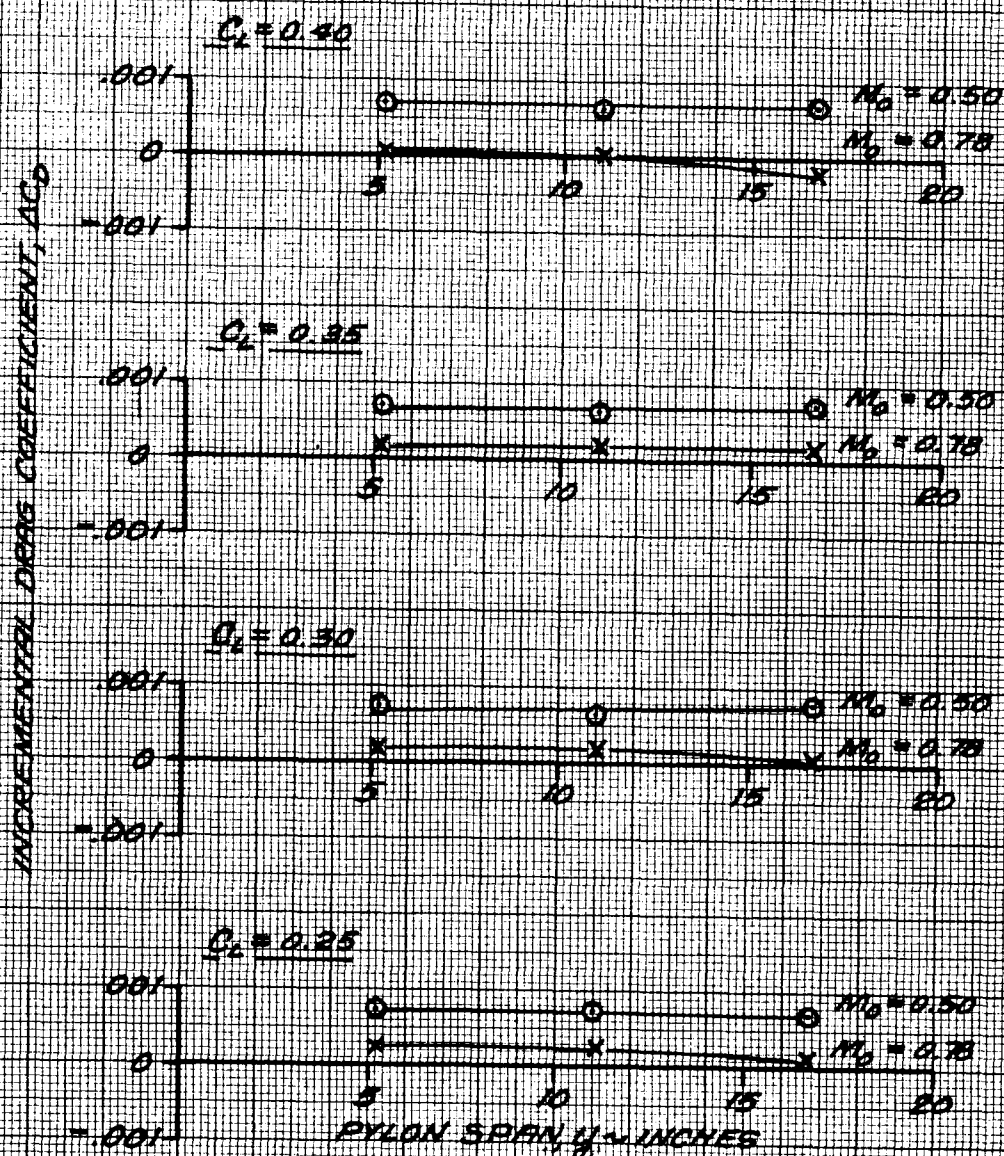


Figure 8.- Effect of pylon span on incremental drag coefficient for reflex nacelle.

$C_L = .35$

SYMBOL	CONFIGURATION
○	NACELLES AND PYLONS OFF
△	PRODUCTION NACELLE
□	11.0-INCH REFAN NACELLE
×	5.2-INCH REFAN NACELLE

NOTE: SUBSCRIPT "PEAK, N/P OFF" REFERS TO PEAK PRESSURE COEFFICIENT WITH NACELLES AND PYLONS OFF.

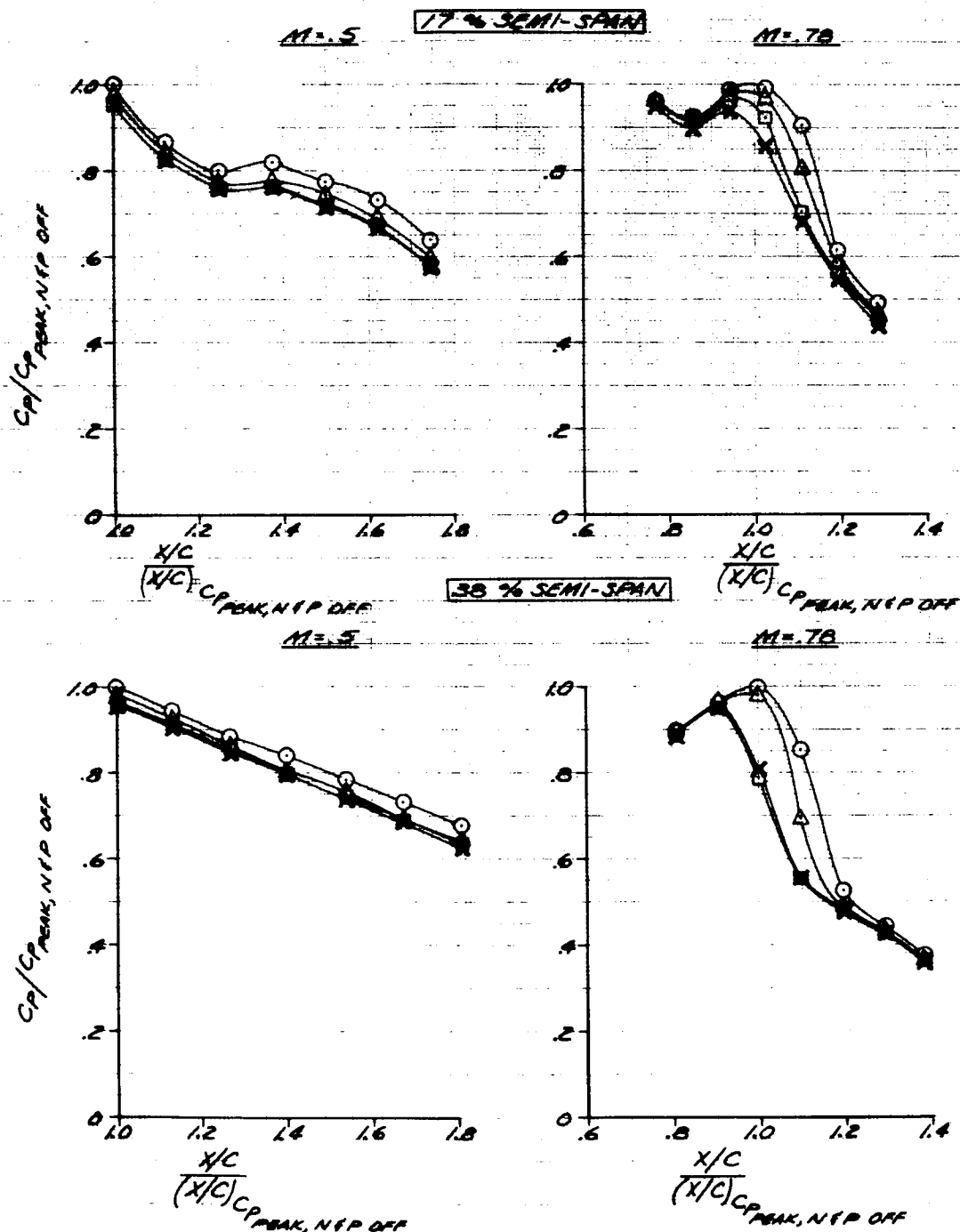


Figure 9.- Wing upper-surface pressure distributions.

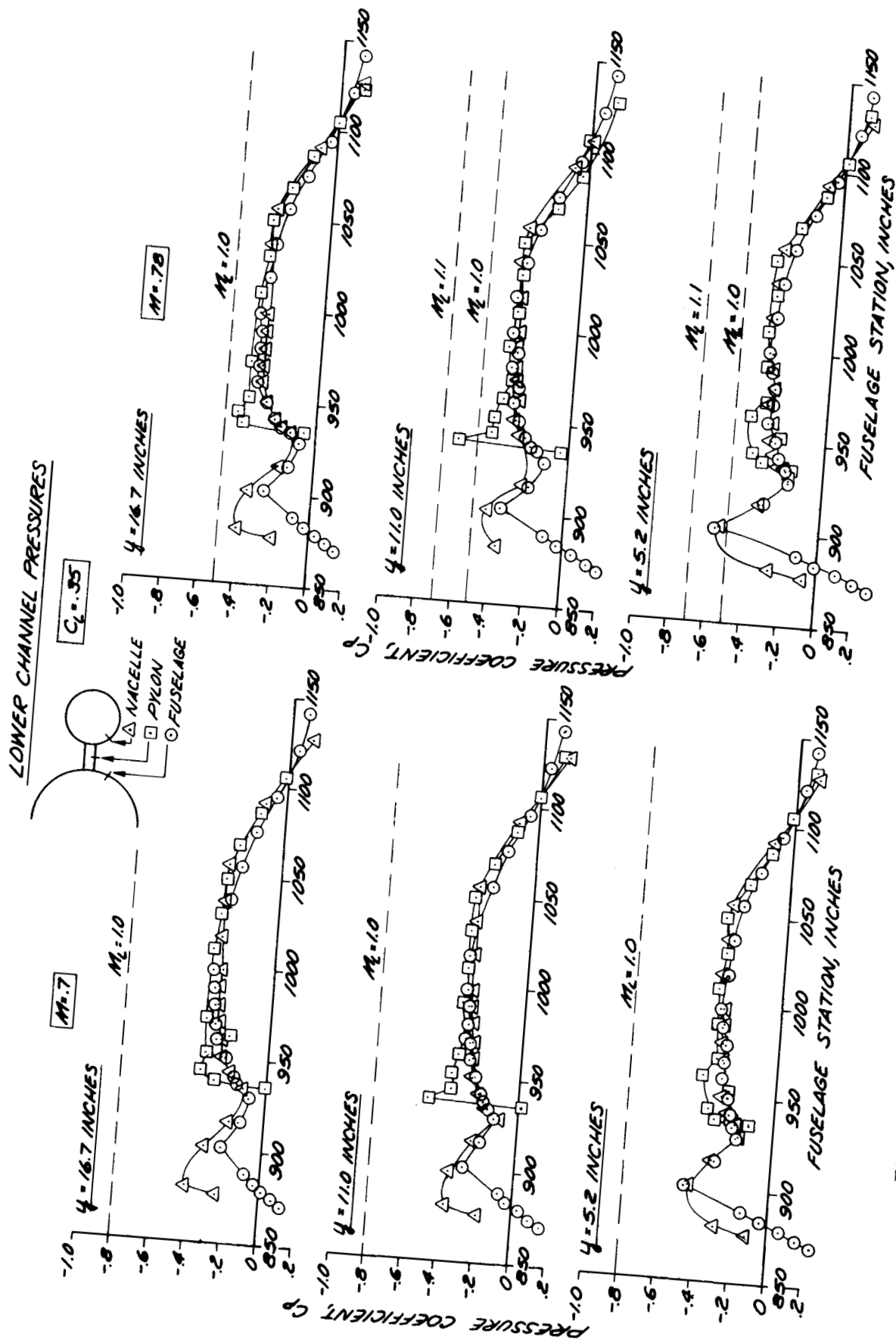


Figure 10.- Nacelle/pylon/fuselage lower-channel pressure distributions.

UPPER CHANNEL PRESSURES

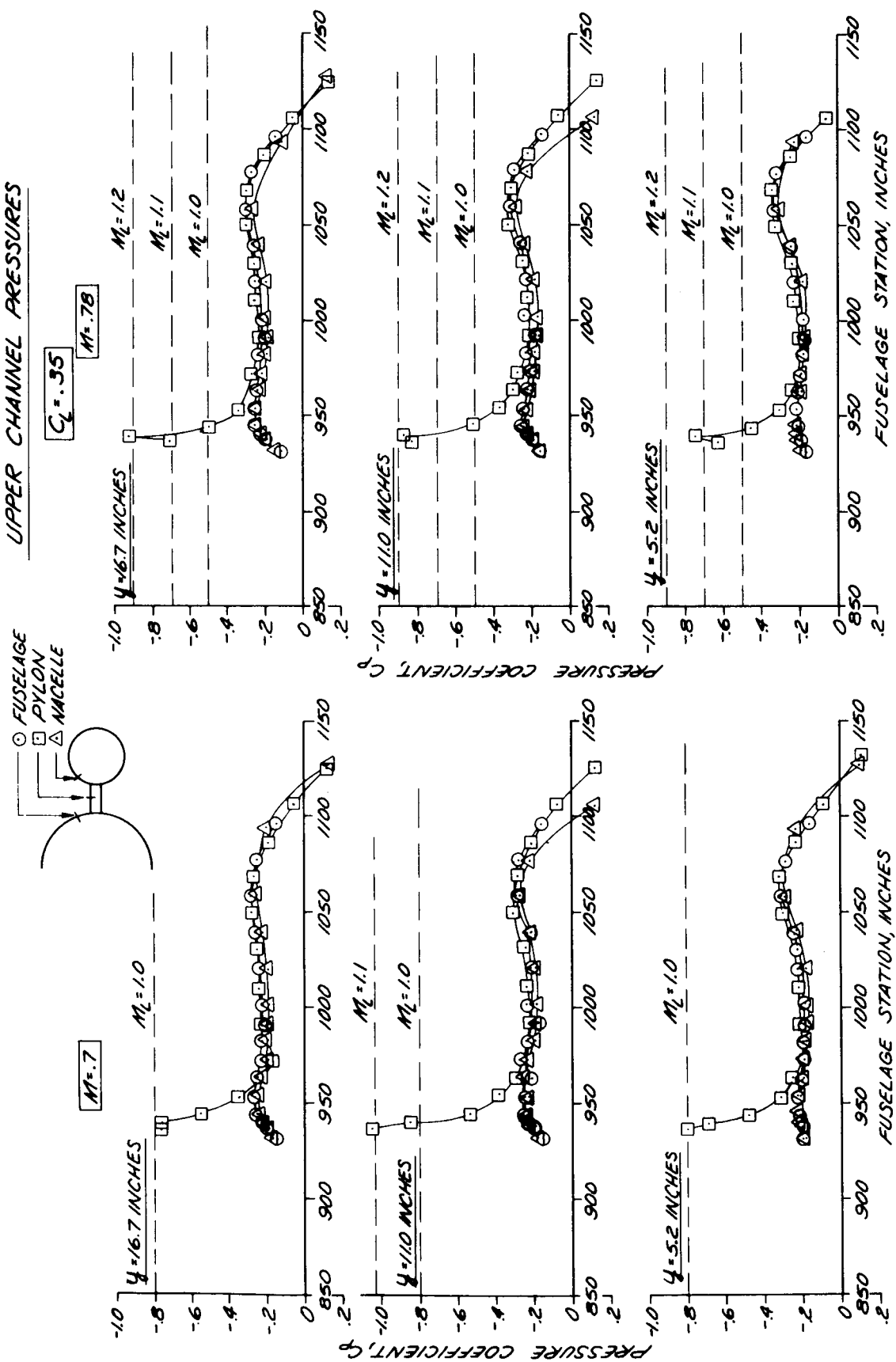


Figure 11.- Nacelle/pylon/fuselage upper-channel pressure distributions.

1. Report No. NASA CR-721219		2. Government Accession No.		3. Recipient's Catalog No.	
4. Title and Subtitle The Effects on Cruise Drag of Installing Refan-Engine Nacelles on the McDonnell-Douglas DC-9				5. Report Date May 1973	
				6. Performing Organization Code	
7. Author(s) J. T. Callaghan, J. E. Donelson, and J. P. Morelli				8. Performing Organization Report No. MDC J5948	
9. Performing Organization Name and Address Douglas Aircraft Company Long Beach, California				10. Work Unit No.	
				11. Contract or Grant No. NAS 3-16814	
12. Sponsoring Agency Name and Address National Aeronautics and Space Administration Washington, D. C. 20546				13. Type of Report and Period Covered Contractor Report	
				14. Sponsoring Agency Code	
15. Supplementary Notes Project Manager, Arthur Medierous Research Center, Cleveland, Ohio NASA/Lewis					
16. Abstract A high-speed wind tunnel test has been conducted in the NASA Ames 11-foot wind tunnel during January 1973 to determine the effect on cruise drag for installing larger JT8D Refan engine nacelles on the McDonnell Douglas DC-9. Drag data and wing- and nacelle/pylon/fuselage-channel pressure data are presented. Reduced pylon spares, required to minimize effects of the nacelle installation on low-speed deep stall, were investigated. The reduced-span pylons resulted in no adverse interference effects. At typical cruise Mach numbers the measured penalty for the Refan installation was less than estimated due to a favorable effect of the larger entering engine stream tube suppressing the wing upper-surface velocities with subsequent wing compressibility drag reduction. Channel pressures show no shock waves or boundary layer separations.					
17. Key Words (Suggested by Author(s)) DC-9 refanned nacelle high speed pylon span				18. Distribution Statement	
19. Security Classif. (of this report) Unclassified		20. Security Classif. (of this page) Unclassified		21. No. of Pages 39	
				22. Price*	

* For sale by the National Technical Information Service, Springfield, Virginia 22151